Acta Crystallographica Section F
Structural Biology and Crystallization Communications
ISSN 1744-3091

Expression, crystallization and preliminary X-ray studies of the immunoglobulin-like domain 3 of human palladin

Wenxue Liang,[a] Haitao Yang,[b,c] Xiaoyu Xue,[b,c] Qiuhua Huang,[a] Mark Bartlam[b,c]* and Saijuan Chen[a]*

[a]State Key Laboratory of Medical Genomics and Shanghai Institute of Hematology, Rui Jin Hospital Affiliated to Shanghai Second Medical University, Shanghai 200025, People's Republic of China, [b]Tsinghua–IBP Joint Research Group for Structural Biology, Tsinghua University, Beijing 100084, People's Republic of China, and [c]National Laboratory of Biomacromolecules, Institute of Biophysics (IBP), Chinese Academy of Sciences, Beijing 100101, People's Republic of China

Correspondence e-mail: bartlam@xtal.tsinghua.edu.cn, sjchen@stn.sh.cn

Received 23 March 2006
Accepted 4 May 2006

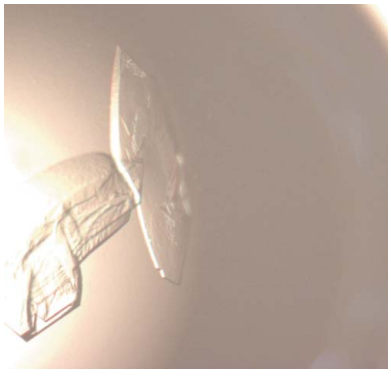

© 2006 International Union of Crystallography
All rights reserved

Palladin is a member of the recently discovered palladin/myotilin/myopalladin family, the members of which associate with α-actinin. Palladin may play important roles in actin stress-fibre formation, cell adhesion and migration. The immunoglobulin-like domain 3 of human palladin has been overexpressed in *Escherichia coli* and crystallized suitable for X-ray crystallographic study. Crystals have been obtained using the vapour-diffusion method and belong to space group $P2_1$. X-ray diffraction data were collected in-house to 1.8 Å resolution from a single crystal. The unit-cell parameters are a = 40.9, b = 33.3, c = 34.8 Å, β = 90.3°. One molecule was predicted to be present in the asymmetric unit.

1. Introduction

Palladin, together with myotilin and myopalladin, is a member of a novel subfamily of cytoskeletal immunoglobulin-like domain-containing proteins. All of them serve as scaffolds that regulate actin organization. Palladin co-localizes with α-actinin in stress fibres, focal adhesions, cell–cell junctions and embryonic Z-lines. It is ubiquitously expressed in embryonic tissues and downregulated in certain adult tissues in the mouse (Parast & Otey, 2000). Palladin is expressed mainly in smooth muscle and non-muscle and is distributed along microfilaments in a periodic manner consistent with dense regions/bodies (Mykkanen *et al.*, 2001). Increased palladin expression is associated with cytoskeletal reorganization in the NB4 cell line, dendritic cells, trophoblastic cells and astrocytes (Boukhelifa *et al.*, 2003; Luo *et al.*, 2005; Mykkanen *et al.*, 2001; Parast & Otey, 2000). Downregulation of palladin expression by antisense constructs resulted in cytoskeleton disruption and neurite-outgrowth failure (Parast & Otey, 2000).

Palladin has multiple isoforms in tissues and cultured cell lines (Boukhelifa *et al.*, 2001; Mykkanen *et al.*, 2001; Parast & Otey, 2000). Each isoform may have specific functions in certain cell types and developmental status. The largest palladin isoform, with an apparent molecular weight of 200 kDa, has two proline-rich regions and five immunoglobulin-like domains. It is transcribed from the promoter nearest the 5′ end. The sequence and expression patterns of the 200 kDa isoform quite closely resemble those of myopalladin. The most abundant 90–92 kDa isoform has a proline-rich region in the N-terminal half of the molecule and three tandem immunoglobulin-like domains in the C-terminal half, corresponding to immunoglobulin-like domains 3–5 of the 200 kDa isoform. It is transcribed from the middle promoter. The N-terminal of this isoform contains binding sites for vasodilator-stimulated phosphoprotein (VASP) and α-actinin (Boukhelifa *et al.*, 2004). Immunoglobulin-like domains may be involved in protein–protein and protein–ligand interactions. Recent studies on palladin gene knockout mice show that the inactivation of palladin immunoglobulin-like domains 3–5 led to embryonic lethality owing to severe defects in cranial neural tube closure and herniation of the liver and intestine (Luo *et al.*, 2005). No specific function has yet been associated with immunoglobulin-like domain 3. The immunoglobulin-like domains 4–5 of palladin are responsible for the interaction with ezrin (Mykkanen *et al.*, 2001), which may serve as a docking site for various types of proteins and is involved in mechanisms of targeted signalling into cells. Furthermore,

immunoglobulin-like domains 3–5 of myopalladin expressed in cardiac and skeletal muscle have been shown to be required for binding to α-actinin (Bang *et al.*, 2001).

These studies suggest that palladin plays important roles in cellular morphogenesis and cell motility. Determination of the crystal structure will help in understanding the function of palladin immunoglobulin-like domains. In this report, we describe the crystallization and preliminary crystallographic analysis of the immunoglobulin-like domain 3 of human palladin as a prelude to elucidation of its three-dimensional structure.

2. Materials and methods

2.1. Protein expression and purification

The gene sequence encoding the immunoglobulin-like domain 3 of human palladin (residues 770–873 of NP_057165) was amplified using the PCR method with forward primer 5′-CGGGATCCCCTGTGGAAAATGGAATGGCACCATTCTTTGAGAT and reverse primer 5′-CGCTCGAGTCATTGGTTGACAGCCTGTACCAT. The template used was the cDNA of human palladin (GenBank accession No. AF077041). The PCR product was cloned into the pGEX-6p-1 plasmid (Pharmacia) and the resulting recombinant vector was transfected into *Escherichia coli* strain BL21 (DE3). Transformed cells were grown at 310 K in LB medium with 100 mg ml^{-1} ampicillin to an optical density of 0.7–0.9 (OD_{600}) before induction with 0.1 m*M* IPTG for 12 h at 289 K. Cells were harvested and resuspended in lysis buffer [1×PBS (140 m*M* NaCl, 2.7 m*M* KCl, 10 m*M* Na_2HPO_4, 1.8 m*M* KH_2PO_4 pH 7.3), 1 m*M* PMSF, 1 m*M* DTT] and homogenized by sonication. The lysate was centrifuged at 15 000*g* for 30 min to remove cell debris. The supernatant was applied onto a GST affinity column (1 ml glutathione Sepharose 4B) and the contaminant protein was washed away with washing buffer (1×PBS, 1 m*M* DTT, 500 m*M* NaCl). The GST tag was cleaved by PreScission protease overnight at 277 K and the protein with an additional five-amino-acid tag at the N-terminal (-GPLGS-) was then eluted with lysis buffer. The pooled sample was loaded onto a Superdex 75 column (Pharmacia) with buffer *A* (20 m*M* HEPES pH 7.5, 100 m*M* NaCl, 1 m*M* DTT). The purity of the final protein was determined to be greater than 95% by SDS–PAGE analysis and further dynamic light-scattering analysis showed that 70–80% of the protein remains as monomers in solution.

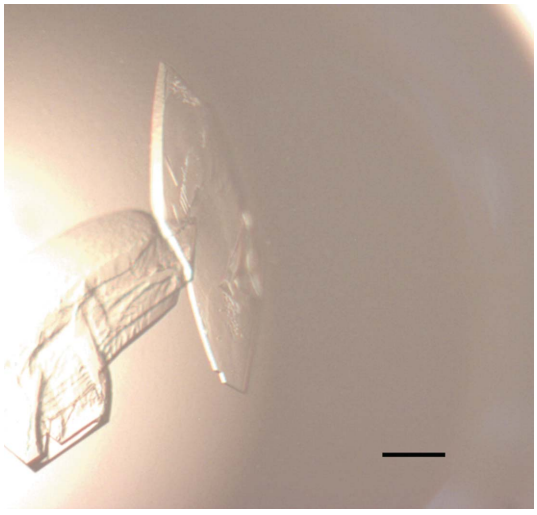

Figure 1
Typical crystals of the immunoglobulin-like domain 3 of human palladin grown by the hanging-drop method in 0.1 *M* HEPES pH 7.5, 15%(*v*/*v*) PEG 10 000. The scale bar represents 0.1 mm.

2.2. Crystallization

The purified protein was concentrated to 15–20 mg ml^{-1} in buffer *A* using a 5K Filtron ultrafiltration membrane. Protein concentrations were determined by absorbance at 280 nm. Hampton Research Crystal Screen kits were used to screen crystallization conditions and then fine-tuned. Each drop was formed by mixing equal volumes (1.5 µl) of protein solution and reservoir solution and was allowed to equilibrate *via* vapour diffusion over 200 µl reservoir solution at 291 K. The protein was diluted with buffer *A* to 10 mg ml^{-1} prior to mixing with the reservoir solution. The protein sample was centrifuged at 14 000*g* for 10 min to remove any precipitate prior to setting

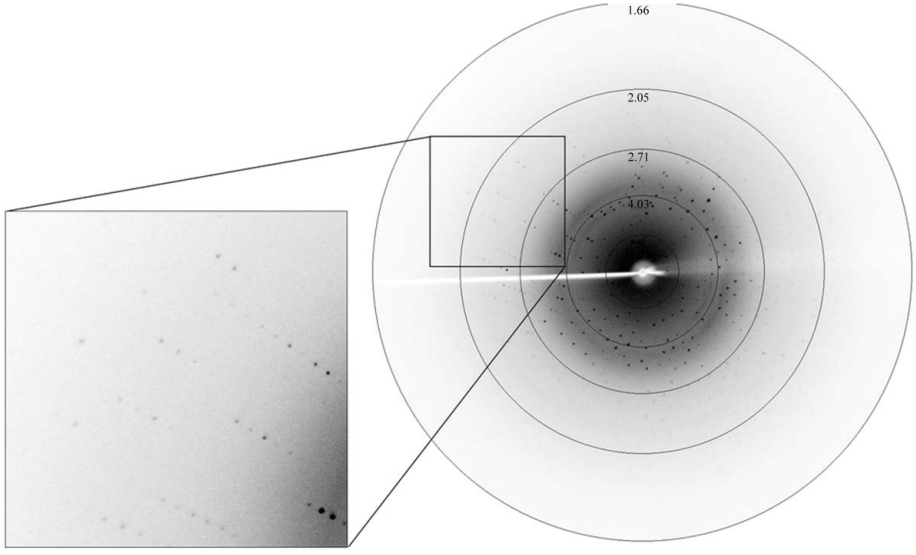

Figure 2
A typical X-ray diffraction pattern from a crystal of the immunoglobulin-like domain 3 of human palladin. The diffraction image was collected on a MAR Research MAR 345 image-plate detector. An enlarged image is shown on the left.

Table 1
Data-collection and processing statistics.

Values in parentheses are for the highest resolution shell.

Space group	$P2_1$
Unit-cell parameters (Å, °)	a = 40.9, b = 33.3, c = 34.8, β = 90.3
Wavelength (Å)	1.5418
Resolution range (Å)	50.0–1.8 (1.86–1.80)
Observed reflections	60734
Unique reflections	16012
Completeness (%)	93.8 (90.5)
$\langle I/\sigma(I)\rangle$	13.5 (7.0)
$R_{\rm merge}$† (%)	5.1 (19.1)

† $R_{\rm merge} = \sum_h \sum_i |I_{h,i} - I_h| / \sum_h \sum_i I_{h,i}$ for the intensity (I) of i observations of reflection h.

up crystallization trials. Several conditions yielded crystals within one week and the best condition was judged to be 20% PEG 4000, 10% 2-propanol, 0.1 *M* HEPES pH 7.5. However, the resulting crystals diffracted poorly. Crystallization conditions were optimized from the initial hit condition by varying the concentration of precipitants and using different types of PEG. The optimum crystals were obtained after two weeks from 200 µl reservoir solution containing 0.1 *M* HEPES pH 7.5, 15% PEG 10 000 (Fig. 1).

2.3. Data collection and processing

Data collection was performed in-house with a Rigaku RU2000 rotating copper-anode X-ray generator operating at 48 kV and 98 mA (Cu $K\alpha$; λ = 1.5418 Å) and a MAR 345 image-plate detector. The crystal was mounted on a nylon loop and flash-cooled in a cold nitrogen-gas stream at 100 K using an Oxford Cryosystems cryostream with the reservoir solution as a cryoprotectant. The oscillation range, exposure time and crystal-to-detector distance were 1° per frame, 5 min per frame and 120 mm, respectively. Data processing was performed using the program *DENZO* and data sets were scaled and merged using *SCALEPACK* (Otwinowski & Minor, 1997).

3. Results and discussion

We obtained initial crystals using a solution containing 20% PEG 4000, 10% 2-propanol, 0.1 *M* HEPES pH 7.5, but the crystals were not suitable for X-ray diffraction. Crystals grown from an optimized reservoir solution (0.1 *M* HEPES pH 7.5, 15% PEG 10 000) were more suitable for X-ray diffraction and diffracted to 1.8 Å resolution (Fig. 2). The crystals belong to space group $P2_1$, with unit-cell parameters a = 40.9, b = 33.3, c = 34.8 Å, β = 90.3°. From a total of 60 734 observed reflections, 16 012 independent reflections were measured. Assuming the presence of one molecule in an asymmetric unit, the solvent content is calculated to be 37.9% and the Matthews coefficient ($V_{\rm M}$) is 2.0 Å^3 Da^{-1}. Selected data statistics are given in Table 1. The structural and functional analysis of human palladin will be published elsewhere.

We are grateful to Zihe Rao for generous advice and support. This work was supported by Project 973 of the Ministry of Science and Technology (grant No. 2004CB520801).

References

Bang, M. L., Mudry, R. E., McElhinny, A. S., Trombitas, K., Geach, A. J., Yamasaki, R., Sorimachi, H., Granzier, H., Gregorio, C. C. & Labeit, S. (2001). *J. Cell Biol.* **153**, 413–427.
Boukhelifa, M., Hwang, S. J., Valtschanoff, J. G., Meeker, R. B., Rustioni, A. & Otey, C. A. (2003). *Mol. Cell. Neurosci.* **23**, 661–668.
Boukhelifa, M., Parast, M. M., Bear, J. E., Gertler, F. B. & Otey, C. A. (2004). *Cell Motil. Cytoskeleton*, **58**, 17–29.
Boukhelifa, M., Parast, M. M., Valtschanoff, J. G., LaMantia, A. S., Meeker, R. B. & Otey, C. A. (2001). *Mol. Biol. Cell*, **12**, 2721–2729.
Luo, H., Liu, X., Wang, F., Huang, Q., Shen, S., Wang, L., Xu, G., Sun, X., Kong, H., Gu, M., Chen, S., Chen, Z. & Wang, Z. (2005). *Mol. Cell. Neurosci.* **29**, 507–515.
Mykkanen, O. M., Gronholm, M., Ronty, M., Lalowski, M., Salmikangas, P., Suila, H. & Carpen, O. (2001). *Mol. Biol. Cell*, **12**, 3060–3073.
Otwinowski, Z. & Minor, W. (1997). *Methods Enzymol.* **276**, 307–326.
Parast, M. M. & Otey, C. A. (2000). *J. Cell Biol.* **150**, 643–656.